Study of Membrane-Induced Conformations of Substance P: Detection of Extended Polyproline II Helix Conformation

ARTICLE *in* THE JOURNAL OF PHYSICAL CHEMISTRY B · MARCH 2011

Impact Factor: 3.3 · DOI: 10.1021/jp1101253 · Source: PubMed

3 AUTHORS, INCLUDING:

Esteve Padrós
Autonomous University of Barcelona
102 PUBLICATIONS **1,340** CITATIONS

SEE PROFILE

THE JOURNAL OF PHYSICAL CHEMISTRY B

ARTICLE

pubs.acs.org/JPCB

Study of Membrane-Induced Conformations of Substance P: Detection of Extended Polyproline II Helix Conformation

Arash Foroutan,[†] Tzvetana Lazarova,[*,†] and Esteve Padrós[*]

Unitat de Biofísica, Departament de Bioquímica i de Biologia Molecular, and Centre d'Estudis en Biofísica, Facultat de Medicina, Universitat Autònoma de Barcelona, 08193 Bellaterra, Barcelona, Spain

ABSTRACT: We study the conformation of substance P (SP), a ligand of neurokinin 1 receptor, and its analogue [Trp8]SP in membrane-mimetic media to provide further insights into membrane−ligand interactions and the factors determining and modulating the peptide structure. CD data revealed that the neuropeptide attains α-helical fold in negatively charged SDS micelles and DMPG liposomes but not in zwitterionic DMPC. The fluorescence experiments reported that the Trp side chain of [Trp8]SP inserts into the hydrophobic core of the SDS micelles and DMPG liposomes but faces the DMPC hydrophilic region, indicating that electrostatic interactions between membrane and SP are essential for the α-helical fold. Formation of extended polyproline II (PPII) helical structure in aqueous solutions and in submicellar concentrations of SDS and DMPC liposomes was confirmed by comparing CD spectra at increasing temperatures. Moreover, in all conditions where PPII conformation was detected, the Trp was totally exposed to the bulk. The PPII structure may be vital for recognition processes of SP by neurokinin receptors.

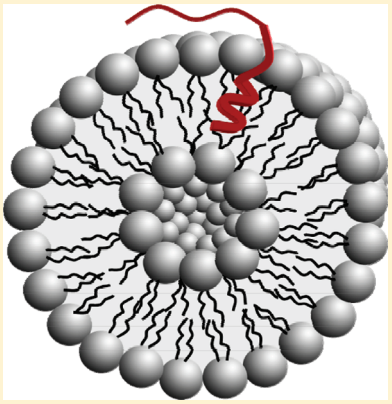

INTRODUCTION

Ligand binding is an essential step for the functioning of the most diverse and largest protein family of G-protein coupled receptors (GPCRs). After agonist binding GPCRs activate, allowing the cytoplasmatic domain of the receptor to interact with a specific G-protein and to transmit the signal.[1] Defects in ligand−GPCR interactions affect inter- and intracellular signaling communications and are considered as one of the main reasons for many human diseases.[2,3] Consequently, the molecular basis of ligand recognition by GPCRs is a topic of primary interest in cellular recognition studies and for understanding how these proteins do work. Despite the biological importance of GPCR proteins, knowledge about the forces and mechanisms governing ligand−receptor interactions is still on the infancy level.[4] Recent determination of the high-resolved structures of three members of the GPCR family including rhodopsin, β2-adrenergic, and adenosine A_{2A} receptors advanced notably our understanding on how these proteins work as signaling molecules.[5,6] However, considering the substantial evidence that GPCR exist in numbers of flexible active conformations, these structures offer only a static view of a single-protein conformation.[1,7] Indeed, for the ligand−receptor studies the high-resolution structure of the ligand bound to the receptor is one of the most desirable. Yet, because of the ligand−receptor complexity, other strategies attempting the structural characterization of the active biological form of the ligand are desirable.

Among the tachykinin family, substance P (SP) is the most potent natural ligand of neurokinin 1 (NK1) GPCR receptor.[8,9] It is a positively charged neuropeptide, composed by 11 amino acids (Arg1-Pro2-Lys3-Pro4-Gln5-Gln6-Phe7-Phe8-Gly9-Leu-10-Met11-NH_2), and is believed to be involved in several physiological processes in the central and peripheral nervous system.[10−12] The implication of SP agonist in stress mechanisms, mood/anxiety regulation, and some neurodegenerative disorders makes it a therapeutically relevant agent. An understanding of how the SP ligand interacts with the NK receptors is essential to permit a rational design of compounds acting selectively at the receptor level.[13]

As suggested by mutagenesis and heterologous expression studies, the binding site of SP is close to the extracellular membrane interface of NK1 receptor, involving residues of the first and second extracellular loop and the second and seventh transmembrane domain.[14−18] Despite the fact that in the several past years SP and NK1 receptor have been extensively studied, the mechanism by which the neuropeptide recognizes its receptor remains elusive. Some authors have proposed that the target cell surface has an important role in the biological activity of SP, either by increasing the ligand concentration at the membrane surface or by inducing and stabilizing its active conformation.[19,20] On the contrary, some other authors believe that lipids may play an important role for the SP storage but most likely are not directly involved in the binding of SP to its receptor.[21] Indeed, membrane-mimetic environments are suitable milieu to obtain insight into the mechanism by which the SP recognizes the receptor. A number of previous reports on the SP structural properties come from molecular dynamics, circular dichroism

Received: October 22, 2010
Revised: February 7, 2011
Published: March 11, 2011

(CD), and nuclear magnetic resonance (NMR) studies. However, most of the molecular dynamics and NMR studies have been performed using methanol, dimethyl sulfoxide, or 2,2,2-trifluoroethanol (TFE) as solvents to mimic the membrane milieu.[22−25] The conformation of SP in micelles and liposomes, two common model systems to mimic the membrane environment, has been more extensively explored by CD, Fourier transform infrared, and recently NMR experiments.[26−30] NMR studies of the micelle-associated structure of SP proposed that the C-terminal tripeptide (Gly-Leu-Met-NH_2) adopts an extended structure while the N-terminal is quite flexible.[31] In the midregion of SP, a conformational equilibrium between α-helical and 3_{10} structures has been proposed,[31,26,32] while other authors have suggested α-helical[33,31] or turn-like structures.[26,34] More recent characterization of SP in phosphatidylcholine vesicles by 2D trNOE NMR spectroscopy reported a well-defined conformation in the last seven C-terminal amino acids consisting of nonstandard turns followed each other in a helix-like manner.[29]

The role of peptide−lipid interactions for the insertion and conformation of SP in the membrane matrix is another area of debate. Using the monolayer technique it was reported that SP inserts into negatively charged 1-palmitoyl-2-oleoyl-*sn*-glycero-3-phosphoglycerol but not into zwitterionic 1-palmitoyl-2-oleoyl-*sn*-glycero-3-phosphocholine.[35,36] The role of the electrostatic interaction for the insertion of SP into bilayer has been questioned by analysis of the binding isotherms, suggesting binding of SP to neutral lipids.[37] CD experiments reported unordered SP structure in phosphatidylcholine but a partially α-helical structure in negatively charged liposomes as well as in sodium dodecyl sulfate (SDS) micelles.[38] Contrary to these reports, an earlier CD work claimed that the conformation of SP is independent of the lipid headgroup type.[33] This view has been lately supported by CD and ^{1}H NMR studies.[26] Although these studies clearly recognize the essentiality of the lipid matrix for insertion, they also reveal that the modes of neuropeptide−receptor interactions and the mechanisms controlling the ligand binding are yet not entirely understood.

In the present work, we study the conformation of SP and its analogue [Trp8]SP (abbreviated SPW) in SDS micelles and liposomes to understand better membrane/neuropeptide interactions and the factors determining and modulating the peptide structure in membrane-mimetic environments. CD experiments were performed to address the questions concerning the SP conformation, while fluorescence spectroscopy was carried out to obtain information about peptide binding and insertion.

MATERIALS AND METHODS

Materials. Monosodium phosphate dihydrate (≥99%), disodium phosphate dehydrate (≥98%), sodium carbonate (≥99%), and sodium hydrogen carbonate (≥99%) were purchased from Merck & Co., Inc. 2,2,2-Trifluoroethanol (TFE) (≥99%), sodium dodecyl sulfate (SDS) (99%), and pyrene (99%) were purchased from Sigma-Aldrich, Inc. 1,2-Dimyristoyl-*sn*-glycero-3-[phospho-rac-(1-glycerol)] (sodium salt) (DMPG) and 1,2-dimyristoyl-*sn*-glycero-3-phosphocholine (DMPC) were purchased from Avanti Polar Lipids, Inc. SP and SPW were purchased from AnaSpec, Inc. The purity of the peptides was >98% as judged by HPLC and further confirmed by mass spectrometry. The lyophilized peptides were stored at −20 °C as solid powders.

Peptides Concentration. The concentration of the peptide solutions was calculated using UV absorption spectroscopy. The molar extinction coefficient (in L $mol^{-1}cm^{-1}$) of the peptides was determined on the basis of the number of aromatic amino acid residues present in the peptides and considering a molar extinction coefficient of Trp and Phe of 5600 (at 280 nm) and 200 M^{-1} cm^{-1} (at 258 nm), respectively.[39] Thus, the molar extinction coefficient calculated for SP and SPW is 400 and 5800 $M^{-1}cm^{-1}$, respectively. The absorption spectra of the peptides were recorded in a 1 cm length quartz cuvette using a UV−vis spectrometer (Varian Cary3 Bio). For all UV spectra an appropriate correction for a nonzero baseline was done. Prior to the measurements, peptide stock solutions (at about 6.7 mg/mL) were dissolved in distilled water.

Evaluation of Critical Micelle Concentration. The critical micelle concentration (CMC) of SDS was evaluated using fluorescence emission spectra of polarity-sensitive dye pyrene, as described previously.[40] The methodology is based on the well-established experimental fact that the fluorescence emission spectrum of monomeric pyrene reflects the polarity experienced by the probe, as smaller values of the intensities ratio of the third and first vibrational (I_3/I_1) peaks correspond to greater polarity of the probe environment and vice versa.[41] Briefly, a stock solution of 1 mM pyrene in ethanol was made and added to the samples to a final concentration of 2 μM. Fluorescence emission spectra of pyrene were measured in the presence of increasing concentrations of SDS micelles (from 50 μM to 10.0 mM) using a 335 nm excitation wavelength. The CMC of the SDS surfactant alone and in the presence of SP was determined by plotting the ratio of fluorescence emission intensities of I_{385}/I_{374} vibronic bands vs surfactant concentration.

Preparation of Large Unilamellar Vesicles (LUVs). First, a thin lipid film was prepared by dissolving an appropriate amount of lipid in chloroform/methanol (2:1 v/v) and drying it by a rotary evaporation system purged continuously with a steam of N_2. To avoid any presence of some residual organic solvents, the lipid film was kept under high vacuum overnight. Further, the dried lipid film was hydrated in 5 mM phosphate buffer (pH 7.0), keeping it above the phase-transition temperature with vigorous vortexing for at least 30 min. The resulting multilamellar vesicles (MLVs) were freeze−thawed in liquid nitrogen for at least seven cycles. To get LUVs, MLVs were extruded repeatedly 10 times through stacked polycarbonate membrane with a pore size of 100 nm using a Mini Extruder (Lipofast, Avestin, Ottawa, Canada). All liposomes were used immediately after preparation. The size distribution of LUVs was evaluated by an Ultrafine Particle Analyzer (UPA) 150 spectrometer (Microtrac, Montgomeryville, PA).

Fluorescence Emission Measurements. The fluorescence emission measurements were performed on a SLM 8000 spectrofluorimeter operating in the photon-counting mode. In the peptide−micelle binding experiments, fluorescence emission spectra of SPW were monitored from 300 to 480 nm using a 280 nm excitation wavelength. All spectra were measured at 22 °C with the following parameters: 10 nm/min scanning speed, 4 and 8 nm bandwidth for excitation and emission slits, respectively, and 1 cm path length quartz cuvette. Typically, to increase the signal-to-noise ratio, at least 6 scans were accumulated and averaged. All spectra were corrected by subtracting blank spectra of the corresponding solutions without peptide and for dilution.

CD Measurements. The far-UV CD spectra (190−260 nm) of the peptides were recorded on a Jasco (Tokyo, Japan) J-715 spectropolarimeter. The instrument was calibrated prior to each measurement. All measurements were carried out at 22 °C using a 1 mm path length quartz cuvette. Each spectrum was obtained after an averaging of at least four scans. Dynode voltage values were simultaneously recorded with CD spectra, and only the CD spectra being in the linear range of the dynode values were further considered for analysis of the data. The usual peptide concentration used in all experiments was 100 μM unless otherwise mentioned. Before final ellipticity calculation, all spectra were corrected by subtraction of the respective spectra obtained from peptide-free samples (containing only membrane mimicking environments). The instrument parameters applied were 2.0 nm bandwidth for all the slits, 10 nm/min scanning speed, 1 data point per nanometer, and 2 s response time. The CD intensity of the peptides is expressed in terms of the mean residue molar ellipticity (MRE) according to the following equation (in deg cm^2 dmol^{-1})

$$[\theta] = \theta_{obs}/10 \times Lcn$$

where θ_{obs} is the observed circular dichroism (in mdeg), L is the optical path length (in cm), c is the peptide concentration (in M), and n is the number of residues.

The percentage of α-helix was calculated according to the method of Chen et al.,[42] assuming that the residue ellipticity at 222 nm is exclusively due to α-helix (in deg cm^2 dmol^{-1})

$$\text{percentage of } \alpha\text{-helix} = [\theta]_{222}/[\theta]_{222}^{max}\left(1 - \frac{k}{n}\right)$$

where $[\theta]_{222}$ is the observed mean residue ellipticity at 222 nm, $[\theta]_{222}^{max}$ is the theoretical mean residue ellipticity for a helix of infinite length (−39 500 at 222 nm), n is the number of residues, and k is a wavelength-dependent constant (2.57 for 222 nm).

Since this method is extremely sensitive to the peptide concentration, complementary estimation of SP secondary structural conformation was done using R1 ($\theta_{195}/\theta_{208}$) and R2 ($\theta_{222}/\theta_{208}$) parameters. These R1 and R2 parameters are independent of peptide concentration and have been shown to be useful in comparing relative helicity for closely related peptides when a two-state α-helix/random-coil equilibrium exists.[43] It has been shown that for a random structure, R1 should be positive and R2 close to zero, while in a highly helical state, R1 should be close to −2 and R2 approach 1.[43,44] The CD spectra of SP and SPW peptides were independent of the peptide concentration (60−100 μM), supporting the idea that the peptides are inserted as monomers into the micelles and liposomes.

RESULTS

SP Conformation in Aqueous Solution. Identification of the Polyproline II (PPII) Conformation. Consistent with earlier reported data, the CD spectrum of SP in water displays a single negative peak at 195 nm, assigned to a random coiled conformation of the peptide.[26] When SP was dissolved in neutral (phosphate pH 7.0) or alkaline (carbonate pH 10.7) buffers, the shape of the spectrum did not change much compared to that in water, presenting a strong negative peak at about 195 nm and a small positive peak at about 222 nm (Figure 1A). The overall features of these spectra and, in particular, the presence of the

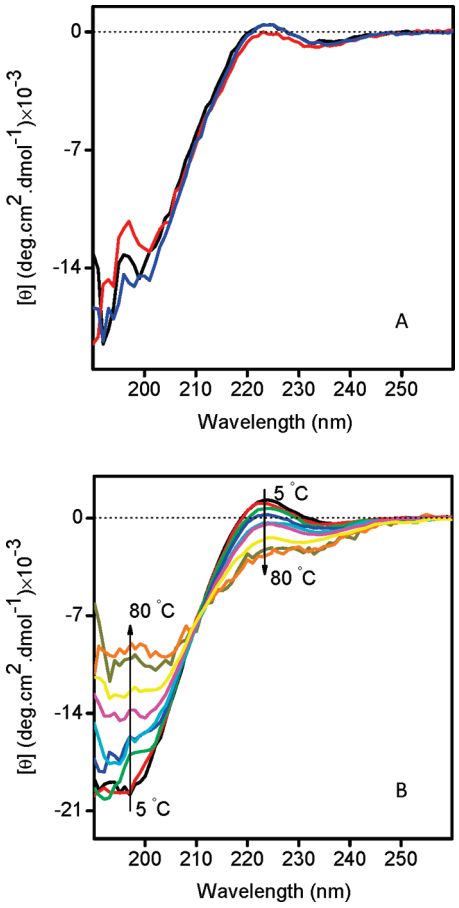

Figure 1. (A) Representative far-UV CD spectra of 100 μM SP in 5 mM Pi buffer pH 7.0 (black line), 3 mM carbonate buffer pH 10.7 (red line), and distilled water (blue line). (B) CD spectra of 100 μM SP in 5 mM Pi buffer pH 7.0 at the following temperatures: 5, 10, 15, 22, 30, 37, 50, 70, and 80 °C.

weak positive band in the near UV range reproduces closely the features of a left-handed helical PPII structure, characterized by a strong negative band around 206 nm (amide $\pi-\pi^*$ transition) and a weak positive band near 225 nm (n$-\pi^*$ transition).[45−47] Because of the spectral similarity of random coil and PPII structures the latter one can be easily mistaken for random coil, and as a result its presence has been often neglected.[47] A typical characteristic of the extended helical PPII structure is its deficiency in intramolecular hydrogen bonds, distinctive for other regular secondary conformations such as α-helix or β-sheets.[48] This makes PPII indistinguishable from an irregular backbone structure using ^{1}H NMR spectroscopy, an otherwise powerful method for conformational analysis.[49] On the other hand, CD spectroscopy so far is widely recognized as the most reliable methodology for identification of this conformation.[46,50] In particular, since PPII helical conformation is more populated at low temperatures, analysis of CD spectra at different temperatures is a relevant approach to discern between unordered and PPII conformations.[46,50] The CD spectra of SP in phosphate buffer, pH 7.0, as a function of the temperature presented in Figure 1B show that the positive band at 208 nm greatly decreases with increasing temperature, thus providing strong evidence for the existence of PPII conformation. Importantly, the changes of both bands are completely reversible upon

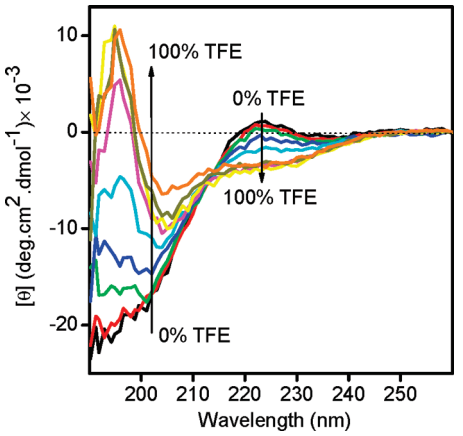

Figure 2. CD spectra of 100 μM SP in TFE/H_2O mixtures of different ratios. The spectra were recorded in distilled water and in 5%, 10%, 15%, 20%, 30%, 40%, 70%, and 100% TFE (v/v). All spectra were collected at 22 °C.

temperature decrease. In addition, the temperature-induced changes in the ellipticity of both bands generate an isoelliptic point at about 211 nm, indicating an equilibrium between unordered and PPII conformations.

Secondary Structure Characterization of SP in the Presence of TFE. To determine the intrinsic helical propensity of SP we carried out experiments in the presence of different concentrations of TFE, known to stabilize α-helical structure in peptides.[51−53] In water and in the presence of less than 15% (v/v) TFE the far-UV CD spectra of SP exhibit a negative peak around 196 nm (Figure 2). Above 30% (v/v) TFE the spectra undergo significant changes and two negative peaks around 208 and 222 nm and a positive peak around 195 nm showed up, indicative of formation of α-helical structure. A further increase of the TFE amount in the mixture results in enhancement of α-helical fold of the peptide, and finally, at concentrations higher than 30% (v/v) TFE it reaches a plateau. The presence of an isodichroic point at about 212 nm implies that the neuropeptide adopts mainly two conformational states. SP follows the same pattern of secondary structural changes with increasing TFE in TFE/phosphate buffer mixtures, pH 7.0. A slightly lower helicity was observed in pure TFE solution than in the TFE/phosphate mixture (data not shown), due to the effect of the salts present in the buffer, as confirmed by comparison with TFE/water experiments.

Secondary Structure Characterization of SP in SDS. To determine the SP conformation(s) in a membrane-mimetic environment, we first analyzed the CD spectra of the neuropeptide in the presence of SDS micelles, a system widely used in structural studies of membrane active peptides.[54,55] In particular, the SDS surfactant was chosen because of 2 reasons: the low turbidity and light scattering of SDS micelles[56,57] and to corroborate our results with previous NMR studies of SP, which generally have been carried out in organic and SDS micelles.[28,31]

In the presence of 10 mM SDS micelles, pH 7.0, highly above the critical micelle concentration (CMC) determined in the buffer (see Figure 4), the CD spectra of SP consist of two negative peaks at 208 and 222 nm, indicating an α-helical conformation (Figure 3A). The structural transition from extended PPII helical structure in aqueous solutions to α-helical in SDS micelles raises the question of how the peptide environment

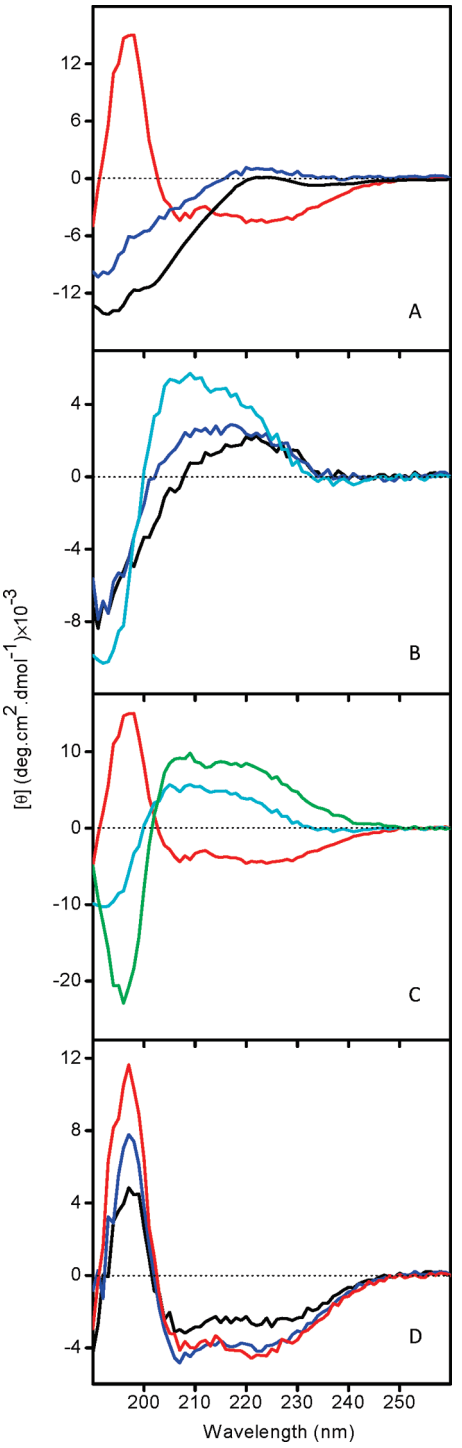

Figure 3. CD spectra of 80 μM SP in (A) 5 mM Pi buffer pH 7.0 (black line) and with 0.2 (blue line) or 10 mM (red line) SDS added. (B) Using 0.4 (black line), 0.6 (blue line), and 0.8 mM (aqua line) SDS. (C) Difference spectrum (green line) calculated by subtraction of the CD spectrum of 80 μM SP in 10 mM SDS (red line) from that in 0.8 mM SDS (aqua line). (D) Using 1.4 (black line), 1.6 (blue line), and 3 mM (red line) SDS. All spectra were collected at 22 °C.

controls and stabilizes these two different conformations. To address this question, we measured CD spectra of SP in SDS solutions below and above the CMC (Figure 3). In the absence

dx.doi.org/10.1021/jp1101253 |J. Phys. Chem. B 2011, 115, 3622–3631

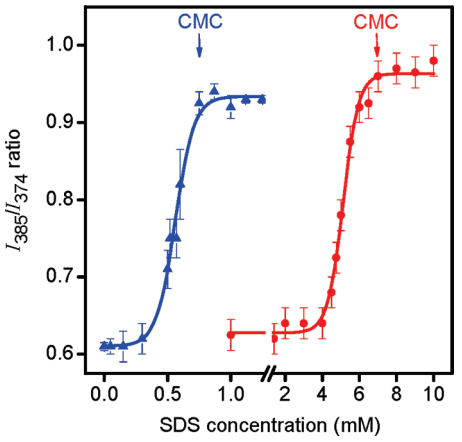

Figure 4. Fluorescence intensity ratio of the third (385 nm) and first (374 nm) vibronic peaks of 2 μM pyrene (I_{385}/I_{374}) in 5 mM Pi buffer pH 7.0, alone (red circles) and in the presence of 25 μM SP (blue triangles) as a function of increasing concentration of SDS from 0 to 10 mM. λ_{exc} was set at 335 nm, and each sample was recorded as an average of 3 emission scans.

and at low (0.2 mM) SDS concentrations the peptide adopts mainly PPII conformation, as judged by the strong negative peak at about 195 nm and a small positive peak at about 222 nm and confirmed by recording the spectra at different temperatures (Figure 1B). A further increase of SDS but still in the submicellar range (between 0.4 and 0.8 mM) results in a decrease and blue shift of the negative peak (of about 5 nm) and appearance of a weak and variable positive peak in the range of 205−208 nm (Figure 3B). A shift of the CD spectral bands to higher or lower wavelengths has been attributed to differences between secondary and tertiary amides of PPII and/or contribution of other secondary structures.[46] To examine the shape diversities of the CD spectra with varying SDS concentrations we calculated the CD difference spectra. In all cases, the difference spectra obtained by subtracting the CD spectra of SP in the presence of 10 mM SDS (highly above CMC) from that measured in SDS concentrations below CMC exhibit a negative band below 200 nm and a positive one at about 217 nm, indicative of formation of PPII structure (Figure 3C). The temperature-dependent intensity of the spectra shown in Figure 3B further confirmed the presence of extended PPII conformation (data not shown). These findings imply that in the presence of SDS, below and near the CMC, SP forms complex secondary conformations of largely PPII admixed with α-helical. Moreover, the enhancement of these bands with an increase of SDS concentration strongly suggests a rise of the fractional population of SP residues involved in PPII structure formation (Figure 3B). At about 1.4 mM SDS the CD spectrum shows α-helical conformation. Further concentration increases results only in a minor changes in the magnitude of the signal, indicating that the SDS-dependent folding of SP is completed (Figure 3D). This SDS concentration roughly corresponds to a peptide/SDS molar ratio of 0.05/1. Assuming 62 molecules of SDS per micelle[58] it seems unlikely that this structure is influenced by possible peptide−peptide interactions. However, the α-helical fold of the peptide observed in SDS at concentrations below the CMC in buffer makes these results somehow unexpected. It is well known that the CMC values of SDS strongly depend on the ionic strength and on the presence of ions.[59] Taking into account the amphipathic character of the

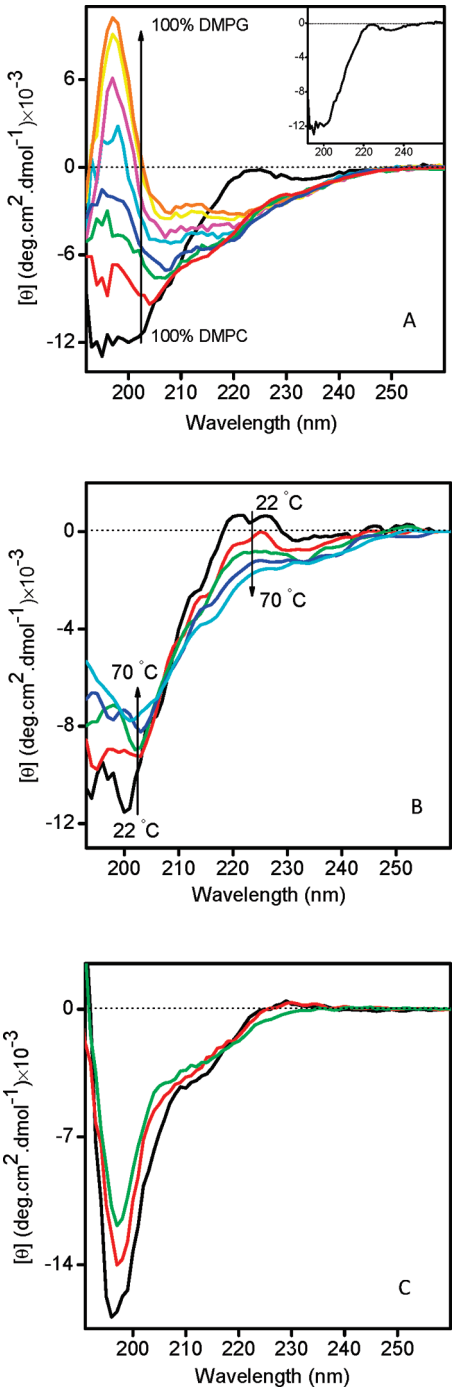

Figure 5. (A) CD spectra of 100 μM SP in phosphate buffer pH 7.0 and 10 mM DMPG/DMPC, prepared at different molar ratios: pure DMPC, 10% DMPG, 15% DMPG, 25% DMPG, 40% DMPG, 50% DMPG, 75% DMPG, and pure DMPG. All spectra were collected at 22 °C. (Inset) CD spectrum of 100 μM SP in 10 mM DMPC. (B) CD spectra of 60 μM SP in DMPC (6 mM) and phosphate buffer pH 7.0, recorded at increasing temperatures: 22, 37, 50, 60, and 70 °C. (C) Difference spectra calculated by subtraction of the CD spectrum of 100 μM SP in 10 mM pure DMPG from that in 10 mM DMPG/DMPC with 10 (black line), 15 (red line), and 25 (green line) mol % of DMPG, pH 7.0.

peptide, we further checked whether the apparent CMC of the surfactant is affected by SP. The plot of the I_{385}/I_{374} ratio of

dx.doi.org/10.1021/jp1101253 |J. Phys. Chem. B 2011, 115, 3622–3631

pyrene bands as a function of SDS concentration (Figure 4) gives an apparent CMC that is about 9-fold lower in the presence of SP, compared to that measured only in buffer. These findings give a rationale for the formation of the α-helical conformation of SP at concentrations above 1.4 mM SDS, as revealed by the CD spectra.

In summary, we conclude that the extended PPII structure is the most populated conformation in SDS monomers. At concentrations near but still below the CMC formation of two fractional conformations, PPII and α-helical, gives rise to distorted CD spectra. Finally, in SDS micelles the α-helical conformation dominates among the other secondary structures.

Lipid-Dependent Folding of SP in Vesicles. Both DMPC and DMPG are structurally similar to the lipid composition in the postsynaptic membranes where NK1 receptor and SP ligand are expressed and functioning.[60] Therefore, LUVs prepared with these lipids mimic most closely phospholipids bilayer in vivo and were used to monitor the membrane-bound conformations of SP.

In zwitterionic DMPC vesicles, the CD spectrum of SP shows the same features as in aqueous solutions, displaying a negative peak around 195 nm and a small shoulder at about 222 nm, suggesting formation of PPII structure (Figure 5A, inset). The temperature-induced changes in the CD spectra of SP in DMPC vesicles unambiguously confirm our assignment to PPII (Figure 5B). Unlikely in DMPC, the CD spectrum of SP in the presence of negatively charged DMPG liposomes exhibits two negative bands at 208 and 222 nm, diagnostic of a dominant α-helical conformation of SP (Figure 5A). Both DMPC and DMPG lipids share a similar length of the acyl chains but differ in their lipid headgroups. To explore the effect of the electrostatic interactions on peptide conformation we measured the spectra of SP in DMPG/DMPC liposomes, prepared with different molar ratios of both lipids (Figure 5A). The presence of DMPG up to 25 mol % in mixed DMPG/DMPC liposomes causes a decrease of the 196 nm band intensity and its shift to 205−208 nm. These alterations are most likely caused by the superposition of CD spectra from different conformations (Figure 5A). Moreover, the small positive shoulder at about 222 nm, seen in pure DMPC, disappears. In the search to identify the structural origin of these spectral changes, we calculated the difference spectra by subtracting the CD spectra of SP in pure DMPG from those in DMPG/DMPC vesicles (Figure 5C). The difference spectra display a strong negative peak at about 195 nm and a small positive peak at about 222 nm, suggesting the presence of PPII conformation. In addition, the intensities of the negative and positive bands illustrate a decrease of PPII content as the DMPG percentage increases. At above 40% (mol/mol) DMPG in DMPG/DMPC liposomes, the CD spectra show α-helical structure, as visualized by the positive band at 196 nm and two negative bands at 208 and 22 nm (Figure 5A). These data demonstrate clearly that the α-helical fold of SP strongly depends on the relative amount of anionic DMPG in the vesicles, since zwitterionic DMPC alone did not induce any α-helix formation, as shown above. Moreover, conformational preference for the α-helical structure in mixed DMPG/DMPC liposomes reflects the favorable electrostatic interaction of the SP with the headgroups of the lipid matrix.

Characterization of the SP Interaction with the Membrane-Mimetic Systems by Fluorescence Spectroscopy. The CD spectra of peptides/membrane-mimetic systems reflect primarily the secondary structural conformation adopted by the peptide, rather than their interactions with the membrane. To seek SP−membrane interactions, we used Trp intrinsic fluorescence, which is highly sensitive to the solvent environment and can serve as a probe to monitor these interactions.[54] In all fluorescence experiments we used SPW, an analogue of SP, in which Phe8 was substituted by Trp. Before using SPW, we tested whether Phe8 substitution for Trp affects the secondary structure of the peptide. Comparison of the CD spectra of SP with those of SPW shows very similar spectral features for both peptides in SDS micelles and DMPG liposomes, except for some subtle differences (Figures 5A, 3A, and 6). Importantly, we found also that SDS in concentrations below the CMC and DMPC above 85% (mol/mol) in DMPG/DMPC vesicles induce conformational changes in SPW similar to those observed in SP, namely, formation of PPII (data not shown). The same structural conformations adopted by SPW and SP allowed us to use the former peptide as a probe for assessing SP−membrane interactions.

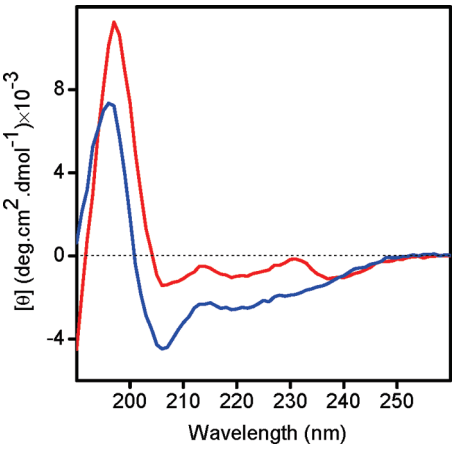

Figure 6. CD spectra of 100 μM SPW in 10 mM SDS (blue line) and in 10 mM DMPG (red line), in phosphate buffer pH 7.0. Spectra were collected at 22 °C.

Figure 7A shows the fluorescence emission spectra of SPW in four different media: aqueous solutions, SDS micelles, and DMPC and DMPG vesicles. In aqueous solutions and DMPC vesicles the fluorescence maximum is located at about 350 nm, indicating that the Trp is totally exposed to the media solution. A significantly blue-shifted maximum to 342 and 337 nm in SDS micelles and DMPG vesicles, respectively, point out the insertion of SPW into the hydrophobic core of these membrane mimetics. Moreover, a larger blue shift and higher Trp intensity of SPW in DMPG liposomes compared to that in SDS micelles suggest a more rigid, hydrophobic environment of Trp side chain in the former environment. The interaction of SPW with SDS surfactant below and above the CMC was monitored by Trp fluorescence emission measurements (Figure 7B). The plot of the titration experiments shows a highly hydrophilic environment of the Trp (with a maximum around 350 nm) in the absence and low SDS concentration range, where the CD spectra revealed an extended PPII-like conformation (Figure 3B). At above 1.2 mM SDS the Trp maximum undergoes a significant blue shift (up to 10 nm), implying insertion of the peptide into the hydrophobic core, which strongly correlates with induction of the α-helical fold observed by CD (Figure 3D).

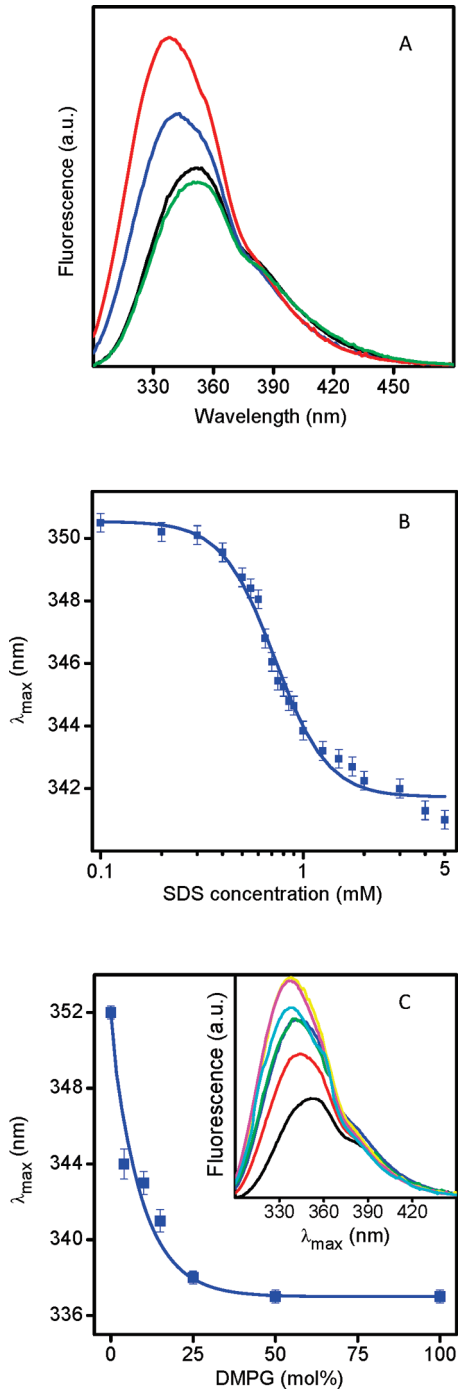

Figure 7. (A) Fluorescence emission spectra of 5 μM SPW in 5 mM Pi buffer (black line) pH 7.0, 10 mM SDS (blue line), 0.5 mM DMPG (red line), and 0.5 mM DMPC (green line). (B) Fluorescence emission λ_{max} of SPW (5 μM) as a function of SDS concentration (pH 7.0). (C) Fluorescence emission λ_{max} of SPW (10 μM) in 1 mM DMPG/DMPC mixtures as a function of different percentages of DMPG: 0%, 4%, 10%, 15%, 25%, 50%, and 100% (mol/mol). (Inset) Fluorescence emission spectra of SPW (10 μM) in DMPG/DMPC mixtures (1 mM) as a function of different molar percentages of DMPG: 0% (black line), 4% (red line), 10% (blue line), 15% (green line), 25% (yellow line), 50% (purple line), and 100% (aqua line). In all cases, λ_{exc} was set at 280 nm.

To evaluate the binding affinity of SPW for the lipid, we measured the Trp fluorescence maximum in liposomes, formed at different DMPG and DMPC molar ratios (Figure 7C). Addition of DMPG up to 15% (mol/mol) results in conformational changes of the peptide segment, involving the Trp residue, as revealed by the blue-shifted Trp maximum (about 10 nm). These data suggest transfer of Trp side chain from a highly hydrophilic in pure DMPC to a more hydrophobic environment in the presence of the anionic DMPG lipid. Above 40% DMPG, the neuropeptide is inserted into the hydrophobic core of the liposomes, as judged by the intensity increase (Figure 7C inset) and strongly blue-shifted Trp maximum (about 15 nm). Therefore, the fluorescence data correlate nicely with formation of the α-helical structure due to the increase of DMPG, as observed by CD measurements (Figure 5A).

It is worth mentioning that in all conditions where CD spectra reported a dominant PPII conformation in the neuropeptide, the fluorescence experiments demonstrated that Trp side chain faces the hydrophilic environment, thus ruling out SPW partition into the hydrophobic core of the micelle or the lipid bilayer. These data are consistent with previous data reporting that peptide segments forming PPII conformation were well exposed to the solvent.[61]

Analysis of the Secondary Structures of SP, Evaluated by CD Experiments. The method of Chen's and co-workers[42] has been widely used for quantitative evaluation of the α-helical content of peptides, and in particular, it has been employed in previous CD studies of SP.[23,26,36] The CD spectra of SP recorded in TFE solvent (Figure 2), SDS micelles (Figure 3), or DMPG and mixed DMPG/DMPC liposomes (Figure 5) are distinct from the spectral signatures for unordered or β-sheet conformations. They represent clearly α-helical conformation, and applying Chen's equation,[42] we calculated the α-helical content of the peptide in these membrane mimetics (Table 1). The α-helical content varies depending on the environment, suggesting genuine differences in the intrinsic helical propensity of SP in different media. The calculated MRE values are in good agreement with a 10−30% α-helical content of SP, previously estimated by CD and Raman spectroscopy measurements.[23,26] From the other side, however, the relatively low MRE values obtained by us and others stress the presence of other conformations being overlooked by Chen's method. We should keep in mind that in any CD spectrum the signal from the α-helical structure usually predominates over the β-turn and unordered ones,[62] resulting in an inability to distinguish between very short helical segments and β-turns.[23] Additionally, any inaccuracy in the determination of peptide concentration could also add some error in estimation of the mean residue ellipticity.[63] Altogether, these considerations reinforce our assumption that the CD spectra of SP most likely represent a superposition of different local conformations, dominated by the most visible and best predicted by CD spectroscopy, the α-helical conformation.

In an attempt to provide further insight into conformations of SP in different membrane-mimetic environments, we calculated R1 ($\theta_{195}/\theta_{208}$) and R2 ($\theta_{222}/\theta_{208}$) parameters, known to be independent of the peptide concentration (Table 1). It is readily seen that R1 is negative in all cases, while R2 is near 1 or >1 in SDS micelles and in DMPG and DMPG/DMPC liposomes. Furthermore, at any TFE concentration in TFE/water mixtures, R2 values are much less than 1. R2 $\ll$ 1 is believed to be diagnostic for short helical segments,[64] the so-called 3_{10}-helical structure, commonly found in short peptides. Thus, we can speculate that the peptide adopts some 3_{10}-helical conformation in the TFE. 3_{10}-Helical structure has been proposed as an

Table 1. Evaluation of α helical content of SP in different membrane-mimetic environments

		DMPG liposomes		SDS micelles		
	70% TFE/water (v/v)	pH 7.0	pH 10.7	pH 7.0	pH 10.7	40% mol DMPG/60% mol DMPC
α-helix %	10.50 ± 1.4	11.5 ± 1.0	13.5 ± 1.5	13.3 ± 0.8	15.3 ± 0.02	16.7 ± 1.4
R1[a]	−1.05 ± 0.12	−1.8 ± 1.0	−2.84 ± 0.4	−4.09 ± 0.8	−4.50 ± 0.02	−0.56 ± 0.04
R2[a]	0.41 ± 0.02	0.90 ± 0.2	1.00 ± 0.02	1.15 ± 0.2	1.20 ± 0.02	0.86 ± 0.04

[a] Definitions of R1 and R2 parameters are given in the experimental section.

intermediate in α-helical formation,[65] though some authors argued that the CD appearance of a 3_{10}-helix is very close to that of an α-helix[66,67] and that the R method to differentiate between both does not work always.[68] Thus, discrimination between 3_{10} and α-helical and quantitative evaluation of extended PPII conformation and β-turn types structures in SP remains a question to be further tested by more sensitive Fourier transform infrared spectroscopy (work in progress in our lab).

DISCUSSION AND CONCLUSIONS

To date, random coil and α-helical conformations have been proposed as the two major types of secondary structures of the neuropeptide SP.[23,36,69,70] In the present work we present CD evidence that α-helical and extended PPII helical structures are the predominant conformations adopted by SP.

On the basis of our CD and fluorescence data we found that the interaction between SP and the membrane mimetics and formation of stable secondary conformations depends strongly on peptide environment. The SP−membrane interactions appear to be rather complex, involving hydrophobic and electrostatic interactions and charge density on the membrane surface.[26] To attest to the impact on each of these components for promotion of a stable peptide conformation we performed experiments in solvents and in two membrane-mimetic environments, liposomes and micelles, varying the head−lipid charge and the concentration of SDS surfactant.

SP is an amphipathic peptide, and it is reasonable to assume that the positively charged N-terminal (involving Arg1 and Lys3) would have a strong impact on the peptide binding through electrostatic interactions with the anionic components of the membrane. Indeed, our experiments support this assumption, demonstrating that the Trp side chain of SPW is inserted into the hydrophobic environment of the negatively charged SDS micelles or DMPG liposomes, but it faces the hydrophilic aqueous region in the zwitterionic DMPC liposomes (Figure 7). The red shift of the Trp emission maximum upon an increase of DMPC percentage in mixed DMPG/DMPC liposomes reflects the transfer of Trp to a more hydrophilic environment and its full exposure to water in pure DMPC. These findings are in agreement with NMR data reporting that SP amides are not protected from solvent exchange in zwitterionic dodecylphosphocholine.[29]

It is worth comparing the fluorescence results with CD data, reporting the conformation of SP in these conditions. As CD data demonstrate, an increase of DMPC percentage in DMPG/DMPC liposomes leads to a decrease of α helicity of SP and in pure DMPC liposomes the extended PPII helical structure appears to be the most preferred and dominant conformation. This indicates that hydrophobic interactions between the peptide and the zwitterionic DMPC liposomes are not sufficient to promote α-helical conformation even though DMPC has the same hydrophobic potential, 12-carbon hydrophobic tail, as DMPG. On the contrary, the negatively charged SDS micelles and DMPG liposomes are able to induce α-helical folding of SP. CD spectra of SP in SDS surfactant below the CMC represent mainly the extended PPII helical conformation (Figure 3). Submicellar SDS is a mixed solvent system, providing a partially organic (low dielectric) and a partially aqueous environment. With increases of SDS concentration the dominant presence of PPII conformation is lost, and when SDS concentration reaches the CMC, the secondary structure of SP is dominated by the α-helical conformation (Figure 3). These findings point out that electrostatic interactions between membrane-mimetic and the charged residues of SP are essential prerequisites for efficient α-helical fold. The electrostatic interactions between peptides and negatively charged lipids have been proposed as driving forces for binding of some peptides to membranes.[54,55] Most likely, the electrostatic interactions are needed to anchor the basic SP to micelle and vesicle interfaces and promote its insertion into the hydrophobic core, thus enabling the hydrophobic interactions required for initiation of the helical formation and stabilization of the α-helix hydrogen-bond network.

Another question addressed in this work was the formation of the extended PPII helix conformation in SP and its biological relevance. CD spectral features of SP in aqueous solutions, submicellar SDS concentrations, and DMPC liposomes definitely show formation of PPII structure, as confirmed by plotting CD spectra over a temperature range (Figures 1B, 3B, and 5B). Actually, CD spectra of SP in aqueous solutions and in zwitterionic lysophosphatidylcholine micelles published previously show spectral features very similar to those reported here, but the authors assigned them to the random coil structures.[22,23,26,33,36,38] Importantly, in all conditions where the CD spectra reported formation of the PPII conformation, the florescence experiments indicate that the Trp side chain has a hydrophilic environment, thus excluding SP partition into the hydrophobic core of the micelles or the lipid bilayer. These results are in accordance with the recognized tendency of PPII helix to form on the surfaces of proteins.[49]

Previously, based on the CD data of SP interaction with SDS and zwitterionic lysophosphatidylcholine micelles, it was claimed that the charge has a pronounced effect on the strength of binding interactions but did not affect the induced conformation of SP.[33] However, the CD spectra presented in Figure 2 of ref 33 clearly show two different peptide conformations, namely, the α-helical structure in SDS micelles and PPII helix in lysophosphatidylcholine micelles. Therefore, a clear influence of the electrical charge can be assumed. On the other hand, NMR experiments reported in the same work show a strong binding of SP with SDS (with some residues inserted) and a weaker binding with the neutral lysophosphatidylcholine (with unaffected Lys NH resonance by the lipid and C-terminal involved in a specific

interaction). These data strongly suggest that the positively charged N-terminal assures a particular spatial topology of the peptide needed for the consequent proper α-helical fold. Therefore, reinterpreting the CD assignments reported in that work,[33] both CD and NMR data strongly support our proposal that electrostatic interactions between the membrane and SP are essential for promoting the α-helical fold. Furthermore, contrary to the α-helical conformation, induction of PPII structure does not need the interaction of the peptide with the membrane, pointing out that PPII formation presumably is dictated by the specific amino acid sequence of SP.

Finally, it is interesting to interpret our findings in the context of SP ligand−NK1 receptor interactions. SP is known to act as a ligand for different NK receptors with different potent activities.[71] On the basis of our data, we hypothesized that the molecular basis for the multiple receptors recognition of SP may be closely related to formation and stability of two major conformations adopted by the peptide: extended PPII helical and α-helical structure. Formation of PPII structure seems an essential structural feature of the SP ligand in targeting different receptors, while the α-helical structure most likely provides the correct conformation of the peptide for receptor signal activation. In the different NK receptors, the segment forming PPII in SP will address the peptide to different binding pockets, due to PPII flexibility, and consequently, the agonist will attain a new conformation that would activate the receptor.

Extended left-handed PPII helical structures have been neglected for years, and only in the last several years growing evidence has accumulated that the PPII conformation is essential for several biological activities, such as molecular recognition, signal transduction, transcription, cell motility, and immune response processes.[47,49] In general, the PPII conformation forms in polypeptides rich in proline, yet even sequences lacking Pro residue can adopt this structure.[61] Pro-rich sequences are known as very common recognition sites involved in signal transduction.[48,72−74] Furthermore, the ligands are found mostly in an extended conformation, when bound to their receptors, as revealed by X-ray and NMR data. Actually, the N-terminus of SP contains two Pro residues forming two short $(XP)_n$ motifs, known to promote PPII helix formation.[49] An additional reason to assume the involvement of the PPII structure in the recognition processes of SP by NK receptors lies in the fact that this regular, periodic structure is very flexible. By adapting the PPII structure SP may easily behave as an "adaptable glove", addressing the SP to the binding pocket in the different NK receptors. Unlike α-helix secondary structure, the PPII helix precludes formation of intramolecular hydrogen bonds,[50] leaving the backbone carbonyl oxygens (and the N−H protons of non-Pro residues) free to participate in hydrogen bonding with interacting receptors at the interface of the peptide−protein complex. As we show here, PPII helix conformation is preformed in the unbound peptide before interacting with the membrane, which presumably guarantees rapid formation of specific peptide−protein complexes.

AUTHOR INFORMATION

Corresponding Author

*T.L.: phone, +34935814504; e-mail, tzvetana.lazarova@uab.cat. E.P.: phone, +34935811870; e-mail, esteve.padros@uab.cat.

Author Contributions

†These authors contributed equally to this work.

ACKNOWLEDGMENT

The authors are grateful to Drs. Víctor Lórenz-Fonfría and Josep Cladera for critical reading of the manuscript and helpful suggestions. This work was supported by a Ministerio de Ciencia e Innovación grant BFU2009-08758/BMC. A.F. is grateful to Ravis Sustainable Development Consulting Engineers Co. (Tehran, Iran) for a fellowship.

ABBREVIATIONS

CD, circular dichroism; CMC, critical micelle concentration; DMPC, 1,2-dimyristoyl-*sn*-glycero-3-phosphocholine; DMPG, 1,2-dimyristoyl-*sn*-glycero-3-[phospho-rac-(1-glycerol)]; GPCR, G-protein coupled receptor; LUV, large unilamellar vesicle; MLV, multilamellar vesicle; MRE, mean residue molar ellipticity; NK, neurokinin; NMR, nuclear magnetic resonance; PPII, polyproline II; SDS, sodium dodecyl sulfate; SP, substance P; SPW or [Trp8]SP, [Trp8]-substance P; TFE, 2,2,2-trifluoroethanol.

REFERENCES

(1) Kobilka, B. K.; Deupi, X. *Trends Pharmacol. Sci.* **2007**, *28*, 397–406.
(2) Shenker, A. *Baillieres Clin. Endocrinol. Metab.* **1995**, *9*, 427–451.
(3) Conn, P. M.; Ulloa-Aguirre, A.; Ito, J.; Janovick, J. A. *Pharmacol. Rev.* **2007**, *59*, 225–250.
(4) Vilardaga, J. P.; Bunemann, M.; Feinstein, T. N.; Lambert, N.; Nikolaev, V. O.; Engelhardt, S.; Lohse, M. J.; Hoffmann, C. *Mol. Endocrinol.* **2009**, *23*, 590–599.
(5) Rosenbaum, D. M.; Rasmussen, S. G.; Kobilka, B. K. *Nature* **2009**, *459*, 356–363.
(6) Costanzi, S.; Siegel, J.; Tikhonova, I. G.; Jacobson, K. A. *Curr. Pharm. Des.* **2009**, *15*, 3994–4002.
(7) Kobilka, B.; Schertler, G. F. *Trends Pharmacol. Sci.* **2008**, *29*, 79–83.
(8) Shimizu, Y.; Matsuyama, H.; Shiina, T.; Takewaki, T.; Furness, J. B. *Cell. Mol. Life Sci.* **2008**, *65*, 295–311.
(9) Van Loy, T.; Vandersmissen, H. P.; Poels, J.; Van Hiel, M. B.; Verlinden, H.; Vanden Broeck, J. *Peptides* **2010**, *31*, 520–524.
(10) Longmore, J.; Hill, R. G.; Hargreaves, R. J. *Can. J. Physiol. Pharmacol.* **1997**, *75*, 612–621.
(11) Murtra, P.; Sheasby, A. M.; Hunt, S. P.; De Felipe, C. *Nature* **2000**, *405*, 180–183.
(12) Covenas, R.; Martin, F.; Belda, M.; Smith, V.; Salinas, P.; Rivada, E.; Diaz-Cabiale, Z.; Narvaez, J. A.; Marcos, P.; Tramu, G.; Gonzalez-Baron, S. *BMC Neurosci.* **2003**, *4*, 3.
(13) Ebner, K.; Sartori, S. B.; Singewald, N. *Curr. Pharm. Des.* **2009**, *15*, 1647–1674.
(14) Fong, T. M.; Huang, R. R.; Strader, C. D. *J. Biol. Chem.* **1992**, *267*, 25664–25667.
(15) Gether, U.; Johansen, T. E.; Schwartz, T. W. *J. Biol. Chem.* **1993**, *268*, 7893–7898.
(16) Huang, R. R.; Yu, H.; Strader, C. D.; Fong, T. M. *Biochemistry* **1994**, *33*, 3007–3013.
(17) Boyd, N. D.; Kage, R.; Dumas, J. J.; Krause, J. E.; Leeman, S. E. *Proc. Natl. Acad. Sci. U.S.A.* **1996**, *93*, 433–437.
(18) Lequin, O.; Bolbach, G.; Frank, F.; Convert, O.; Girault-Lagrange, S.; Chassaing, G.; Lavielle, S.; Sagan, S. *J. Biol. Chem.* **2002**, *277*, 22386–22394.
(19) Schwyzer, R. *EMBO J.* **1987**, *6*, 2255–2259.
(20) Sankararamakrishnan, R. *Biosci. Rep.* **2006**, *26*, 131–158.
(21) Holzemann, G.; Greiner, H. E.; Harting, J.; Barnickel, G.; Seelig, A. *Regul. Pept.* **1993**, *46*, 453–454.
(22) Chassaing, G.; Convert, O.; Lavielle, S. *Eur. J. Biochem.* **1986**, *154*, 77–85.

(23) Williams, R. W.; Weaver, J. L. *J. Biol. Chem.* **1990**, *265*, 2505–2513.
(24) Corcho, F. J.; Salvatella, X.; Canto, J.; Giralt, E.; Perez, J. J. *J. Pept. Sci.* **2007**, *13*, 728–741.
(25) Wymore, T.; Wong, T. C. *Biophys. J.* **1999**, *76*, 1199–1212.
(26) Keire, D. A.; Fletcher, T. G. *Biophys. J.* **1996**, *70*, 1716–1727.
(27) Keire, D. A.; Kobayashi, M. *Protein Sci.* **1998**, *7*, 2438–2450.
(28) Gao, X.; Wong, T. C. *Biopolymers* **1999**, *50*, 555–568.
(29) Auge, S.; Bersch, B.; Tropis, M.; Milon, A. *Biopolymers* **2000**, *54*, 297–306.
(30) Beard, D. J.; Perrine, S. A.; Phillips, E.; Hoque, S.; Conerly, S.; Tichenor, C.; Simmons, M. A.; Young, J. K. *J. Med. Chem.* **2007**, *50*, 6501–6506.
(31) Young, J. K.; Anklin, C.; Hicks, R. P. *Biopolymers* **1994**, *34*, 1449–1462.
(32) Cowsik, S. M.; Lucke, C.; Ruterjans, H. *J. Biomol. Struct. Dyn.* **1997**, *15*, 27–36.
(33) Woolley, G. A.; Deber, C. M. *Biopolymers* **1987**, *26* (Suppl.), S109–121.
(34) Koziej, P.; Mutter, M.; Gremlich, H. U.; Holzemann, G. *Z. Naturforsch. B* **1985**, *40*, 1570–1574.
(35) Seelig, A.; Macdonald, P. M. *Biochemistry* **1989**, *28*, 2490–2496.
(36) Seelig, A.; Alt, T.; Lotz, S.; Holzemann, G. *Biochemistry* **1996**, *35*, 4365–4374.
(37) Pérez-Paya, E.; Porcar, I.; Gómez, C. M.; Pedrós, J.; Campos, A.; Abad, C. *Biopolymers* **1997**, *42*, 169–181.
(38) Wu, C. S.; Hachimori, A.; Yang, J. T. *Biochemistry* **1982**, *21*, 4556–4562.
(39) Campbell, I. D.; Dwek, R. A. *Biological Spectroscopy*; Benjamin-Cummings Publishing Co.: Menlo Park, CA, 1984, pp 61−90.
(40) Domínguez, A.; Fernández, A.; González, N.; Iglesias, E.; Montenegro, L. *J. Chem. Educ.* **1997**, *74*, 1227–1231.
(41) Kalyanasundaram, K.; Thomas, J. K. *J. Am. Chem. Soc.* **1977**, *99*, 2039–2044.
(42) Chen, Y. H.; Yang, J. T.; Martínez, H. M. *Biochemistry* **1972**, *11*, 4120–4131.
(43) Bruch, M. D.; Dhingra, M. M.; Gierasch, L. M. *Proteins* **1991**, *10*, 130–139.
(44) Rizo, J.; Blanco, F. J.; Kobe, B.; Bruch, M. D.; Gierasch, L. M. *Biochemistry* **1993**, *32*, 4881–4894.
(45) Miles, A. J.; Wallace, B. A. *Chem. Soc. Rev.* **2006**, *35*, 39–51.
(46) Woody, R. W. *J. Am. Chem. Soc.* **2009**, *131*, 8234–8245.
(47) Shi, Z.; Chen, K.; Liu, Z.; Kallenbach, N. R. *Chem. Rev.* **2006**, *106*, 1877–1897.
(48) Sreerama, N.; Woody, R. W. *Proteins* **1999**, *36*, 400–406.
(49) Rath, A.; Davidson, A. R.; Deber, C. M. *Biopolymers* **2005**, *80*, 179–185.
(50) Bochicchio, B.; Tamburro, A. M. *Chirality* **2002**, *14*, 782–792.
(51) Nelson, J. W.; Kallenbach, N. R. *Proteins* **1986**, *1*, 211–217.
(52) Nelson, J. W.; Kallenbach, N. R. *Biochemistry* **1989**, *28*, 5256–5261.
(53) Merutka, G.; Stellwagen, E. *Biochemistry* **1989**, *28*, 352–357.
(54) Lazarova, T.; Brewin, K. A.; Stoeber, K.; Robinson, C. R. *Biochemistry* **2004**, *43*, 12945–12954.
(55) Bordag, N.; Keller, S. *Chem. Phys. Lipids* **2010**, *163*, 1–26.
(56) Hoyt, D. W.; Gierasch, L. M. *Biochemistry* **1991**, *30*, 10155–10163.
(57) Garavito, R. M.; Ferguson-Miller, S. *J. Biol. Chem.* **2001**, *276*, 32403–32406.
(58) Thévenot, C.; Grassl, B.; Bastiat, G.; Binana, W. *Colloid Surf. A* **2005**, *252*, 105–111.
(59) le Maire, M.; Champeil, P.; Moller, J. V. *Biochim. Biophys. Acta* **2000**, *1508*, 86–111.
(60) O'Brien, J. S.; Sampson, E. L. *J. Lipid Res.* **1965**, *6*, 537–544.
(61) Rucker, A. L.; Creamer, T. P. *Protein Sci.* **2002**, *11*, 980–985.
(62) Yang, J. T.; Wu, C. S.; Martínez, H. M. *Methods Enzymol.* **1986**, *130*, 208–269.
(63) Greenfield, N. J. *Methods Enzymol.* **2004**, *383*, 282–317.
(64) Silva, R. A.; Yasui, S. C.; Kubelka, J.; Formaggio, F.; Crisma, M.; Toniolo, C.; Keiderling, T. A. *Biopolymers* **2002**, *65*, 229–243.
(65) Millhauser, G. L. *Biochemistry* **1995**, *34*, 3873–3877.
(66) Miick, S. M.; Martínez, G. V.; Fiori, W. R.; Todd, A. P.; Millhauser, G. L. *Nature* **1992**, *359*, 653–655.
(67) Andersen, N. H.; Liu, Z.; Prickett, K. S. *FEBS Lett.* **1996**, *399*, 47–52.
(68) Sudha, T. S.; Vijayakumar, E. K.; Balaram, P. *Int. J. Pept. Protein Res.* **1983**, *22*, 464–468.
(69) Qi, X. F.; Zhorov, B. S.; Ananthanarayanan, V. S. *J. Pept. Sci.* **2000**, *6*, 57–83.
(70) Prabhu, A.; Malde, A.; Coutinho, E.; Srivastava, S. *Peptides* **2005**, *26*, 875–885.
(71) Harrison, S.; Geppetti, P.; Substance, P. *Int. J. Biochem. Cell Biol.* **2001**, *33*, 555–576.
(72) Chen, Y.; Wallace, B. A. *Biophys. Chem.* **1997**, *65*, 65–74.
(73) Choo, L. P.; Jackson, M.; Mantsch, H. H. *Biochem. J.* **1994**, *301*, 667–670.
(74) Convert, O.; Duplaa, H.; Lavielle, S.; Chassaing, G. *Neuropeptides* **1991**, *19*, 259–270.